

The influence of the viscosity and different boundary conditions on the dynamics of the 2D subduction models

Alwina Enns¹

Harro Schmeling²

Thorsten W. Becker³

^{1,2}*Institute of Meteorology and Geophysics, J. W. Goethe-University Frankfurt am Main
Feldbergstraße 47, Frankfurt am Main, Germany; e-mail: ¹ enns@geophysik.uni-frankfurt.de, ² schmeling@geophysik.uni-frankfurt.de*
³*IGPP, SIO, UC San Diego, La Jolla CA, USA; e-mail: tbecker@igpp.ucsd.edu*

J
W
G
U



J.W. Goethe-Universität
Frankfurt am Main

Introduction

Subduction influences plate tectonics by modifying the surface area and velocities of plates, and plates connected to slabs move faster than plates without slabs. Most of the subduction zones on Earth show the trench retreat effect, which influences the subduction process and geologic deformation at the surface. The physics of subduction and of trench retreat was investigated by previous numerical and laboratory experiments (e.g. Zhong and Gurnis, 1995; Christensen, 1996; Becker et al., 1999; Fucciello, 2002). The question arises, which role plays the mantle flow and different rheologies for the subduction and for the trench retreat. We introduce 2D subduction models with periodic (e.g. Gottschaldt, 1997) and reflective free slip boundary conditions to investigate the dynamics of the subducting plate and the effect of the mantle flow around the slab. We used the 2D finite difference code FDCON (Schmeling and Marquart, 1991), which solves the conservation equations of mass, momentum and energy.

1 Models

The models include the following assumptions:

1. No overriding plate
2. No phase changes
3. Plastic deformation of the lithosphere at shallow depth according to the Byerlee law $\tau_{\max} = (a\sigma_n + b) \cdot \lambda$, where σ_n is normal stress at the weakest existing fracture plane, in the models σ_n is assumed to be equal to the lithostatic pressure $P_{\text{lith}} = \rho g z$; $a = 0.6$ and $b = 60$ MPa are constants found experimentally by Byerlee (1978) for the depths < 40 km; $\lambda = 1 - P_{\text{por}}/P_{\text{lith}}$ is the factor due to the pore pressure, P_{por} is the pore pressure

1.1 Models with power law rheology

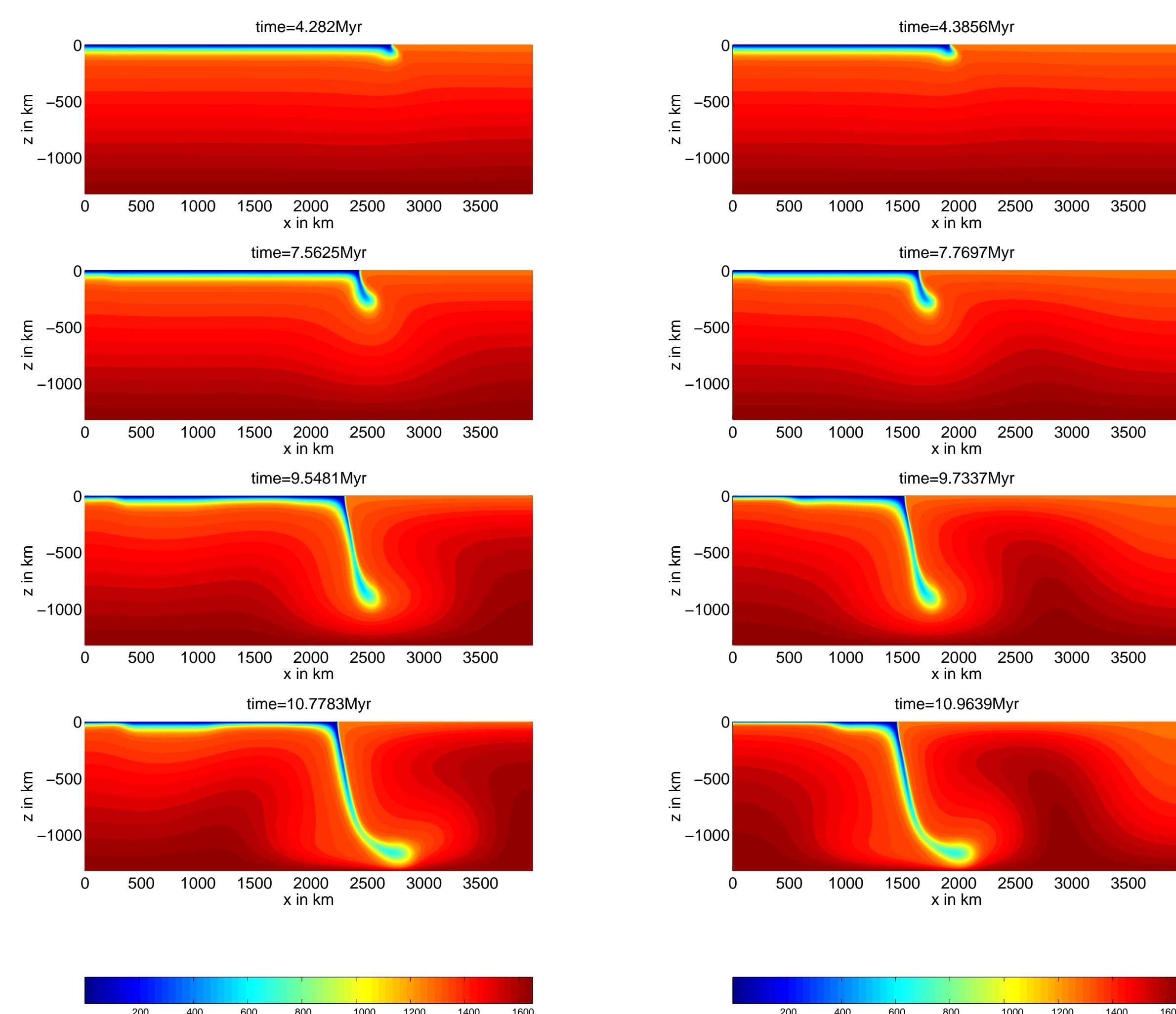
1. Viscosity in the mantle and in the lithosphere according to power law rheology (e.g. Tetzlaff and Schmeling, 2000) $\eta = A \exp((E_a + PV_a)/RT) \tau_{\text{II}}^n$ with $A = 1.103^{16} \text{MPa}^n \text{s}$, $E_a = 535 \text{kJ/mol}$ as activation energy, P as pressure, R as gas constant, T as temperature, τ_{II} as second invariant of deviatoric stress tensor, $n = 3.6$ power law exponent
2. Initial temperature profile with the error function in the lithosphere and an adiabat in the mantle
3. Weak zone in the left upper corner to decouple the lithosphere from the box side
4. Buoyancy due to the compositional density contrast and due to the temperature differences

1.2 Isotherm models

1. Visco-plastic rheology at shallow depth and viscous rheology at greater depth
2. Composition-dependent viscosity
3. Viscosity jump between upper and lower mantle at 660 km by a factor of 50

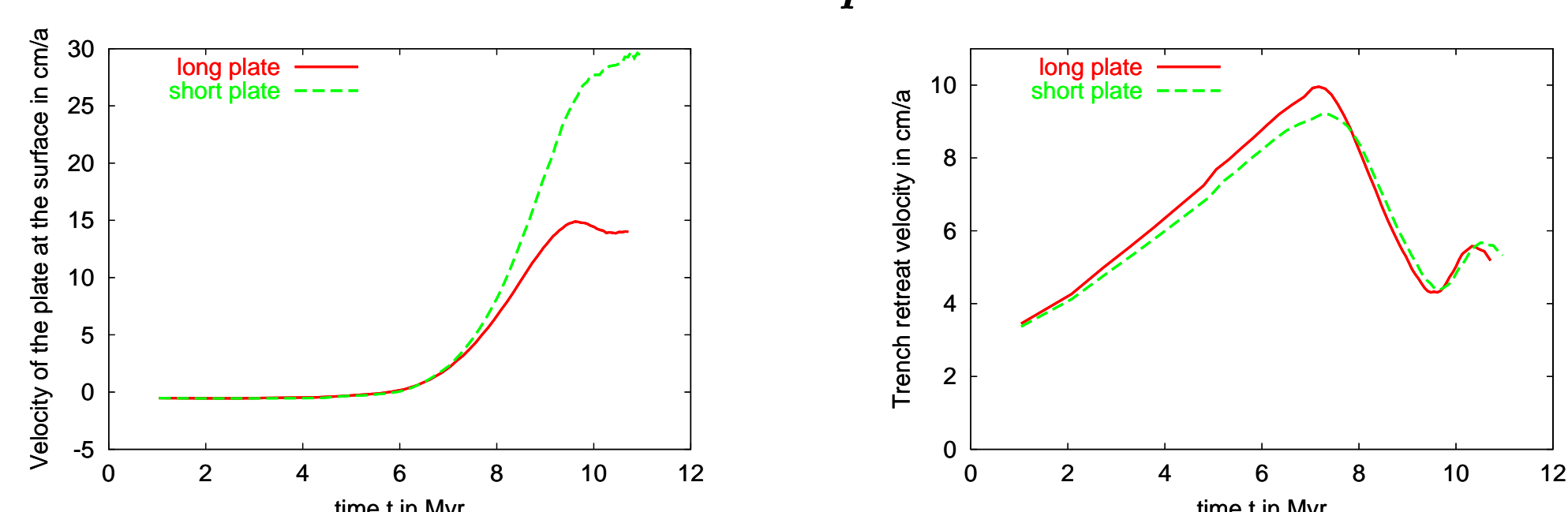
The plastic rheology in the isotherm models and in the models with power law rheology allows the plate to decouple from the top of the model box. The density of the models was advected with the tracer approach. We employed 800×2400 tracers, and filled the $1320 \text{ km} \times 3960 \text{ km}$ model box with 101×301 gridpoints. The grid resolution for the temperature field was four times higher. The viscosity in the models with power law rheology is truncated by 10^{21} Pa s as lower and by 10^{23} Pa s as upper limit.

2 Models with power law rheology



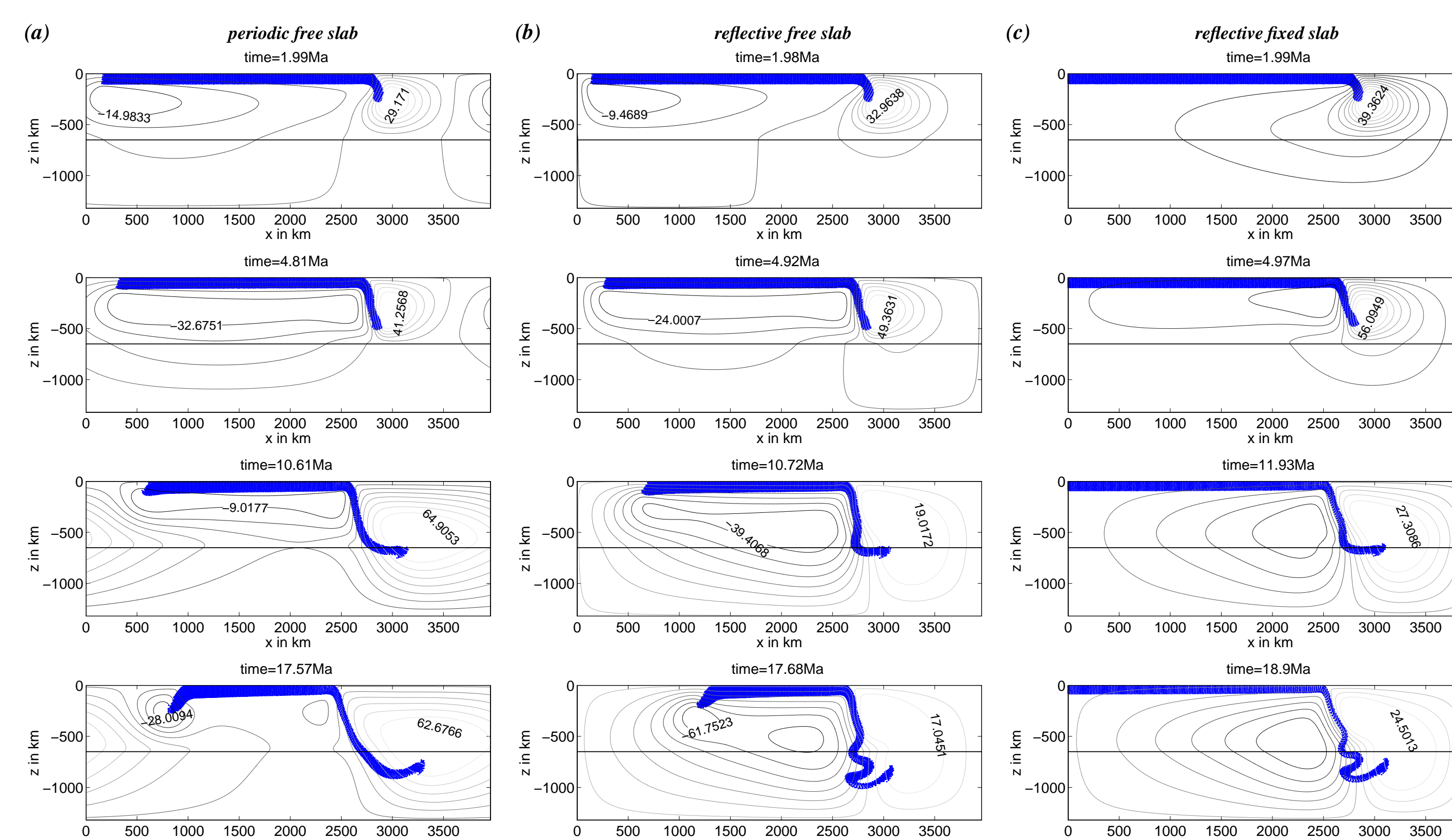
The figures show snapshots of the temperature fields in $^{\circ}\text{C}$ for the models with plates of different lengths. The density of the mantle is $\rho_m = 3200 \text{ kg/m}^3$ and that of the lithosphere is $\rho_{\text{lith}} = \rho_{\text{mantle}} + 50 \text{ kg/m}^3$. The thickness of the lithosphere is $d = 90 \text{ km}$.

Subduction parameters

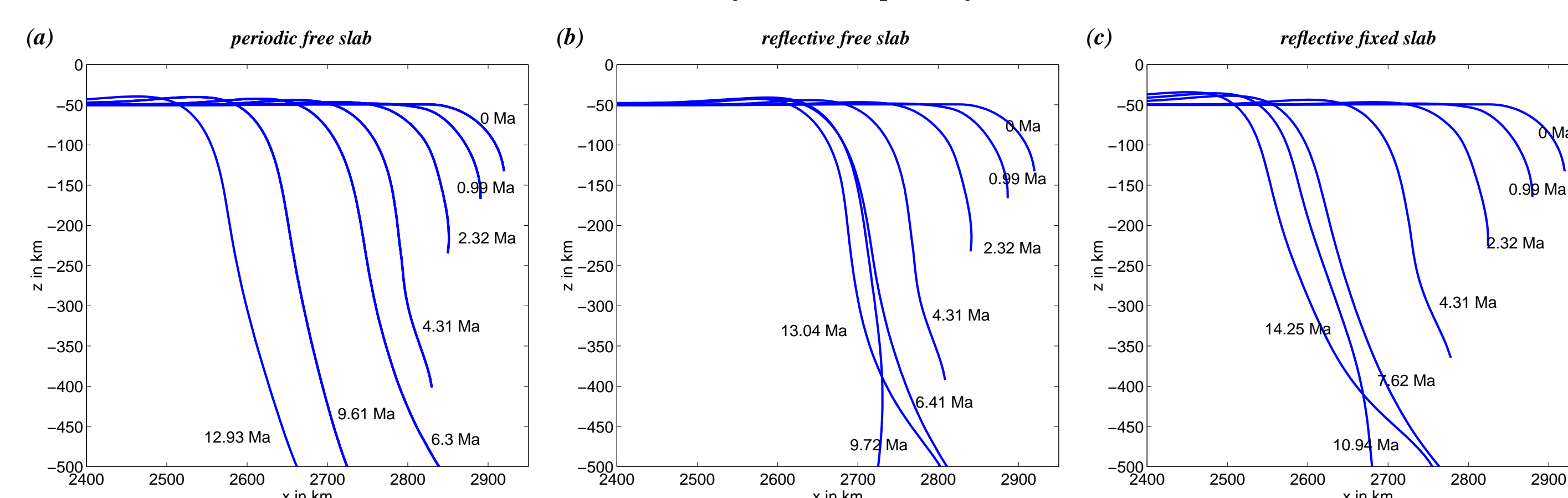


3 Isotherm models with slab viscosity $\eta_{\text{lith}} = 100 \cdot \eta_{\text{um}}$

Snapshots of the models with different boundary conditions



Time evolution of the middle plane of the slab



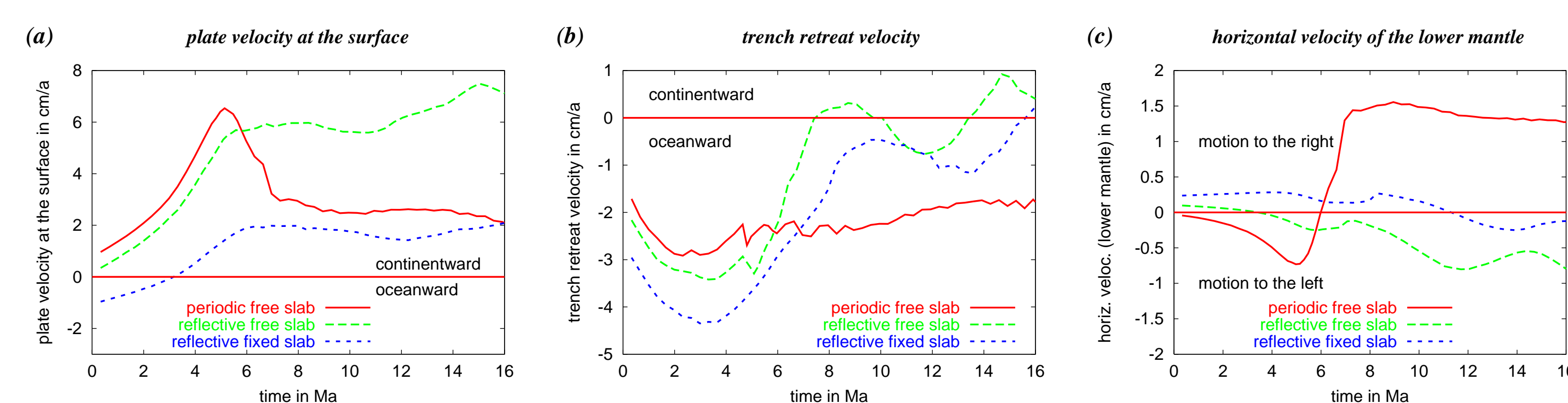
The figures show the model with periodic boundary conditions (BCs) free slab, (a), the model with reflective BCs free slab, (b), and model with reflective BCs fixed slab, (c). Only the marker in the lithosphere are plotted. The following values for viscosity and density were used in the models above:

upper mantle: viscosity $\eta_{\text{um}} = 10^{20} \text{ Pa s}$, density $\rho_{\text{um}} = 3200 \text{ kg/m}^3$

lower mantle: viscosity $\eta_{\text{lm}} = 50 \cdot \eta_{\text{um}}$, density $\rho_{\text{lm}} = \rho_{\text{um}}$

lithosphere: viscosity $\eta_{\text{lith}} = 100 \cdot \eta_{\text{um}}$, density $\rho_{\text{lith}} = \rho_{\text{um}} + 50 \text{ kg/m}^3$, thickness $d = 99 \text{ km}$

Subduction parameters



Results (figures above):

1. Decrease of subduction velocity in the models with stratified viscosity compared to the models with homogeneous mantle
2. Slowdown of the slab after its interaction with the lower mantle
3. Ability of the slab in the periodic BCs model to induce a net horizontal flow in the lower mantle
4. Nearly constant trench retreat velocity throughout of the model run for periodic BCs
5. Decreasing trench retreat velocity after slab/660 km interaction for reflective BCs
6. Folding of the reflective BCs slabs at the 660 km due to the flow confinement
7. Alternating trench motion velocities after slab penetration into the lower mantle for reflective BCs due to folding
8. Fastest rollback of the reflective BCs fixed slab initially, which is overtaken by rollback of the periodic BCs free slab finally

Conclusions

1. Slabs are able to induce a net lower mantle flow (e.g. O'Connell et al., 1991) only for periodic BCs
2. The presence of the lower mantle decreases the subducting velocity and the velocity of the trench retreat
3. The confined mantle flow leads to the stronger folding of the slabs
4. The effect of folding at the 660 km boundary can be observed as a change in the rate of trench retreat
5. For the accelerating stage of subduction the trench retreat occurs predominantly due to plate bending (Ribe, 2001)
6. The models with power law rheology show very fast subduction and trench retreat velocities

References

- Christensen, U. R., The influence of trench migration on slab penetration into the lower mantle, *Earth Planet. Sci. Lett.*, *140*, 27–39, 1996.
- Tetzlaff, M. and Schmeling, H., The influence of olivine metastability on deep subduction of oceanic lithosphere, *Phys. Earth Planet. Inter.*, *120*, 29–38, 2000.
- Zhong, S. and Gurnis, M., Mantle convection with plates and mobile, faulted plate margins, *Science*, *267*, 838–842, 1995.